Available online at www.sciencedirect.com

ScienceDirect

Biomedical Journal

journal homepage: www.elsevier.com/locate/bj

Original Article

Circ_0091579 exerts an oncogenic role in hepatocellular carcinoma via mediating miR-136-5p/TRIM27

Yantao Mao [a,1], Zhigang Ding [b,1], Maozhu Jiang [c], Bo Yuan [b], Yao Zhang [a], Xiaobin Zhang [b,*]

[a] Department of Oncology, Yantaishan Hospital of Shandong Province, Yantai, China
[b] Department of Hepatobiliary Surgery, Dongying People's Hospital, Dongying, China
[c] Oncology Department of Radiotherapy, Yantaishan Hospital of Shandong Province, Yantai, China

ARTICLE INFO

Article history:
Received 23 March 2021
Accepted 23 December 2021
Available online 30 December 2021

Keywords:
Hepatocellular carcinoma
circ_0091579
miR-136-5p
TRIM27

ABSTRACT

Background: Circular RNAs (circRNAs) act as crucial regulators in tumorigenesis. In this study, the working mechanism of circ_0091579 in hepatocellular carcinoma (HCC) progression was investigated.

Methods: The expression of RNA and protein was measured via RT-qPCR and Western blot assay. Cell proliferation ability was analyzed via CCK8, EdU and colony formation assays. Cell migration and invasion abilities were detected via transwell assays. Flow cytometry was applied to assess cell cycle and apoptosis. The target relation between miR-136-5p and circ_0091579 or tripartite motif containing 27 (TRIM27) was certified using dual-luciferase reporter assay. Xenograft tumor model was utilized to assess the role of circ_0091579 in tumor growth *in vivo*. The protein level of Ki67 in tumor tissues was analyzed by immunohistochemistry (IHC) assay.

Results: Circ_0091579 expression was elevated in HCC tissues and cell lines. HCC patients with high circ_0091579 expression displayed low survival rate. Circ_0091579 knockdown suppressed the proliferation, migration, invasion, cell cycle progression and epithelial–mesenchymal transition (EMT) and induced apoptosis of HCC cells. Circ_0091579 acted as a molecular sponge for miR-136-5p, and circ_0091579 silencing-mediated effects were largely overturned by the knockdown of miR-136-5p in HCC cells. MiR-136-5p interacted with the 3′ untranslated region (3′UTR) of TRIM27, and TRIM27 overexpression largely counteracted miR-136-5p overexpression-induced influences in HCC cells. Circ_0091579 sponged miR-136-5p to up-regulate TRIM27 expression in HCC cells. Circ_0091579 silencing suppressed xenograft tumor growth *in vivo*.

Conclusion: Circ_0091579 exhibited an oncogenic role to enhance the malignant potential of HCC cells through mediating miR-136-5p/TRIM27 axis *in vitro* and *in vivo*.

* *Corresponding author*. Department of Hepatobiliary Surgery, Dongying People's Hospital, 317 South 1st Rd., Dongying 257091, China.
E-mail address: ppwmkqm@163.com (X. Zhang).
Peer review under responsibility of Chang Gung University.
[1] Co-author.
http://dx.doi.org/10.1016/j.bj.2021.12.009

At a glance commentary

Scientific background on the subject

CircRNAs have been show to play important regulatory roles in tumorigenesis. Previous studies have suggested that circ_0091579 was up-regulated in HCC tissues, and high level of circ_0091579 predicted the dismal prognosis of HCC patients. However, the working mechanism of circ_0091579 in HCC development remains to be clarified.

What this study adds to the field

We identified the direct interaction between miR-136-5p and circ_0091579 or TRIM27 for the first time. Our data demonstrated that circ_0091579 contributed to HCC development by binding to miR-136-5p to up-regulate TRIM27 level, which provided new potential targets for HCC treatment.

Hepatocellular carcinoma (HCC) is a subtype of liver cancer [1]. Although much effort has been made in HCC treatment, including surgical resection, chemo- or radio-therapy and liver transplantation, the prognosis remains unsatisfactory [2,3]. Illustrating the molecular mechanism behind the tumorigenesis of HCC is urgently needed to improve the prognosis in HCC patients.

Circular RNAs (circRNAs) are a category of loop RNAs that are more stable than linear RNAs [4–6]. Circ_0091579 was up-regulated in HCC, and it exerted an oncogenic role in HCC [7,8]. Circ_0091579 expression was markedly enhanced in HCC, and high level of circ_0091579 was related to worse survival rate in patients [7]. Circ_0091579 accelerated the malignant phenotypes of HCC cells via microRNA-490-5p (miR-490-5p)-dependent regulation of CASC3 [8]. We further explored the working mechanism of circ_0091579 in the carcinogenesis of HCC.

CircRNAs function through acting as microRNA (miRNA) sponges in human malignancies [9]. The dysregulation of miRNAs was closely associated with HCC development. For instance, miR-9-5p facilitated HCC progression via degrading CPEB3 mRNA [10]. MiR-19a-3p and miR-376c-3p contributed to HCC development via SOX6-dependent regulation of Wnt/β-Catenin signaling [11]. MiR-136-5p was reported to be an anti-tumor molecule in HCC by previous articles [12–14]. For example, Liu et al. found that low abundance of miR-136-5p was related to dismal survival rate in patients diagnosed with HCC [14]. The regulatory network of miR-136-5p in HCC progression was further investigated in this study.

MiRNAs regulate the stability and translation of downstream messenger RNAs (mRNAs) through interacting with them [15]. Tripartite motif containing 27 (TRIM27) was initially identified to be an oncogene that was implicated in the activation of RET proto-oncogene via DNA rearrangement [16]. TRIM27 was aberrantly up-regulated in multiple malignancies, containing lung cancer [17], endometrial cancer [18], breast cancer [19] and HCC [20]. Gao et al. found that TRIM27 accelerated the viability, proliferation and motility of HCC cells [20]. Here, TRIM27 was found as a possible downstream partner of miR-136-5p, and the biological effect of circ_0091579/miR-136-5p/TRIM27 signaling cascade in HCC progression was explored.

We analyzed expression pattern of circ_0091579 and explored its biological functions in HCC. Subsequently, possible downstream molecules of circ_0091579 were predicted by bioinformatics analysis, and the working mechanism was explored through conducting rescue experiments.

Materials and methods

Clinical specimens

HCC tumor specimens (n = 70) and corresponding adjacent (ANT) healthy specimens (n = 70) were collected from HCC patients at Yantaishan Hospital of Shandong Province. All subjects involved in this clinical study had signed written informed consents. Committees for Ethical Review of Research at Yantaishan Hospital of Shandong Province granted ethical consent for the clinical study.

Cell lines

Liver immortalized cells THLE-2 and HCC cell lines (HCCLM3, MHCC97H and Huh-7) were purchased from the Cell Bank of the Chinese Academy of Sciences (Shanghai, China). Cells were maintained in Dulbecco's modified Eagle's medium (DMEM; Gibco, Carlsbad, CA, USA) plus 10% fetal bovine serum (FBS, Gibco) and 1% antibiotic solution (Sigma, St. Louis, MO, USA) at the atmosphere of 37 °C and 5% CO_2.

Real-time quantitative polymerase chain reaction (RT-qPCR)

RNA was purified via commercial RNeasy Maxi Kit (Qiagen, Valencia, CA, USA). RNA quality was assessed via the NanoDrop 2000/2000c (Thermo Fisher Scientific, Waltham, MA, USA). Template DNA was synthesized via MicroRNA Reverse Transcription Kit (Applied Biosystems, Foster City, CA, USA) and TaqMan Reverse Transcription Reagents (Invitrogen, Carlsbad, CA, USA). Then RT-qPCR reaction was conducted using SYBR premix Ex TaqII kit (Takara, Dalian, China). Relative abundance was analyzed using the equation of $2^{-\Delta\Delta Ct}$. The primers acquired from Sangon Biotech (Shanghai, China) were shown in Table 2. Glyceraldehyde-3-phosphate dehydrogenase (GAPDH) and U6 were utilized as internal references.

Cell transfection

Small interference RNAs (siRNAs) against circ_0091579 (si-circ_0091579#1, #2, and #3), siRNA negative control (si-NC), short hairpin RNA (shRNA) against circ_0091579 (sh-circ_0091579#1 and sh-circ_0091579#2), shRNA NC (sh-NC), mimics of miR-136-5p (miR-136-5p), miRNA NC (miR-NC), inhibitor of miR-136-5p (anti-miR-136-5p), anti-miR-NC, ectopic expression plasmid of TRIM27 (pcDNA-TRIM27) and pcDNA control (pcDNA-con) were chemically synthesized or constructed by Genepharma (Shanghai, China) and Ribobio

Table 1 The association between circ_0091579 expression and the clinico-pathologic features of hepatocellular carcinoma patients.

Clinical feature	Case (n)	circ_0091579 expression		p
		High (35)	Low (35)	
Age				0.4733
≤55 years	35	19	16	
>55 years	35	16	19	
Gender				0.6313
Female	38	20	18	
Male	32	15	17	
HBV infection				0.1500
Absent	38	22	16	
Present	32	13	19	
TNM stage				0.0084*
I-II	33	11	22	
III	37	24	13	
Tumor size (cm)				0.0008*
≤5	34	10	24	
>5	36	25	11	
Liver cirrhosis				
With	37	18	19	0.8108
Without	33	17	16	

HBV: hepatitis B virus; TNM: tumor-lymph node-metastasis; *$p < 0.05$.

Table 2 Primers in RT-qPCR.

Gene	Sequence (5′-3′)
circ_0091579	TGAGCCAGTGGTCAGTCAAA (forward)
	GTGGAGTCAGGCTTGGGTAG (reverse)
miR-136-5p	TCGGCAGGACTCCATTTGTTTT (forward)
	GCAGGGTCCGAGGTATTC (reverse)
TRIM27	TGCCCCATGAGTGGGATAGA (forward)
	GGATTACAGCCAACAGCCCT (reverse)
U6	GCTTCGGCAGCACATATACTAAAAT (forward)
	CGCTTCACGAATTTGCGTGTCAT (reverse)
GAPDH	TATGATGACATCAAGAAGGTGGT (forward)
	TGTAGCCAAATTCGTTGTCATAC (reverse)

(Guangzhou, China). Lipofectamine® 2000 (Invitrogen) was utilized to transfect these RNA and plasmid into HCC cells.

Cell counting Kit-8 (CCK8) assay

The proliferation ability was assessed via CCK8 commercial kit (Dojindo, Kumamoto, Japan). HCC cells in 96-well plates in quintuplicate were incubated with CCK8 solution (10 μL) for 3 h at indicated time points. The optical density (450 nm) was examined using the microplate reader (Bio-Rad, Hercules, CA, USA).

5-Ethynyl-2′-deoxyuridine (EdU) assay

Cell proliferation capacity was assessed using commercial KeyFluor488 Click-iT EdU Kit (keyGEN Biotech, Jiangsu, China). HCC cells were mixed with 20 μM EdU reagent. Subsequently, HCC cells were immobilized via 4% paraformaldehyde (Sangon Biotech) followed by incubation with 0.5% Triton-X-100 (Sangon Biotech). The nucleus was marked with 4,6-diamino-2-phenyl indole (DAPI) solution (Sigma). Cell images were captured under the fluorescence microscope (Olympus, Tokyo, Japan) at the magnification of 100×. The positive cell rate was analyzed as number of proliferative (EdU^+) cells/number of all ($DAPI^+$) cells × 100%.

Colony formation assay

HCC cells were suspended in culture medium to obtain single-cell suspension, and the single-cell suspension was added into 12-well plates. Colonies were formed during 14-d culture, and the culture medium was replenished every 4 d. Colonies were dyed using 0.1% crystal violet dye liquor (Sangon Biotech).

Transwell assays

Cell motility was measured using commercial Transwell chambers (BD Biosciences, San Jose, CA, USA) coated with (to analyze cell invasion ability) or without (to analyze cell migration ability) Matrigel solution (BD Biosciences). HCC cells were pipetted into the above chambers, with the lower chambers adding 10% FBS-contained medium. After 24-h incubation, HCC cells passed through membrane were marked using 0.1% crystal violet dye liquor (Sangon Biotech). Cell number at 100 × was counted.

Cell cycle analysis

HCC cells were pre-treated with cooled 75% ethanol (Sangon Biotech) for 1 h. RNase A (Thermo Fisher Scientific) was added to remove RNA at 37 °C for 40 min. Subsequently, cells were stained using 500 μL propidium iodide (PI) (Sigma). Cell samples were loaded onto flow cytometer (BD Biosciences), and cell cycle progression was analyzed.

Cell apoptosis analysis

HCC cells in binding buffer (BD Biosciences) were simultaneously mixed with Annexin V-fluorescein isothiocyanate (Annexin V-FITC; BD Biosciences) and PI (BD Biosciences). The apoptosis rate ($FITC^+$ and $PI^{+/-}$) was evaluated by flow cytometer (BD Biosciences).

Western blot assay

Protein concentration in each tube was evaluated via the bicinchoninic acid (BCA) method. Protein samples (30 μg) were separated using sodium dodecyl sulfate-polyacrylamide gel electrophoresis (SDS-PAGE) and then blotted onto polyvinylidene difluoride (PVDF) membrane (Millipore, Billerica, MA, USA). Blocking was applied through mixing the membrane with 5% skimmed milk. Membrane was labeled with primary antibodies (Abcam, Cambridge, MA, USA), including anti-E-Cadherin (ab40772), anti-vimentin (ab92547), anti-N-Cadherin (ab245117), amti-TRIM27 (ab78393) and anti-GAPDH (ab8245). Subsequently, horseradish peroxidase (HRP)-labeled secondary antibody (Abcam) was mixed with the membrane for 2 h. Protein bands were appeared and quantified with the enhanced chemiluminescence chromogenic substrate (Beyotime, Shanghai, China) and ImageJ software (Bio-Rad), respectively.

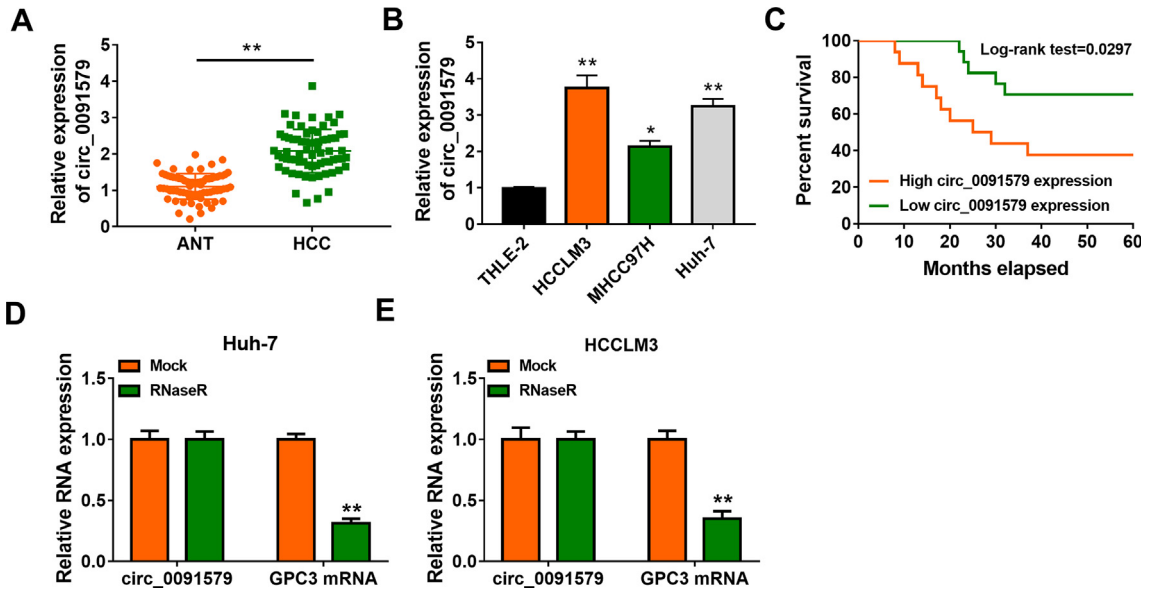

Fig. 1 **Circ_0091579 is dysregulated in HCC tissues and cell lines.** (A) The expression of circ_0091579 was examined in HCC tissues (n = 70) and ANT healthy tissues (n = 70) by RT-qPCR. (B) RT-qPCR was applied to measure the expression of circ_0091579 in three HCC cell lines (HCCLM3, MHCC97H and Huh-7) and human normal liver immortalized cell line THLE-2. (C) HCC patients were divided into high circ_0091579 expression group (n = 16) and low circ_0091579 expression group (n = 17) with the median level of circ_0091579 expression as the cutoff. These patients were followed up for five years, and the survival rate was analyzed. (D and E) Circ_0091579 is derived from the back-splicing of its host gene GPC3. The circular structure of circ_0091579 was tested by exonuclease RNase R, and its linear form GPC3 was used as the control. *$p < 0.05$, **$p < 0.01$.

Subcellular fractionation

The cytoplasmic RNA and nuclear RNA were prepared via commercial Cytoplasmic and Nuclear RNA Purification Kit (Norgen Biotek, Thorold, Canada). The expression level of circ_0091579 was determined via RT-qPCR.

Dual-luciferase reporter assay

The binding relation between miR-136-5p and circ_0091579 or TRIM27 was predicted by CircInteractome (https://circinteractome.irp.nia.nih.gov/) and TargetScan (http://www.targetscan.org/).

The gene fragment of circ_0091579 or TRIM27, possessing the wild-type putative binding sites with miR-136-5p, was constructed into pmirGLO vector (Promega, Madison, WI, USA). Meanwhile, the mutant type luciferase reporter plasmid of circ_0091579 or TRIM27, including mutant complementary sequence with miR-136-5p, was also constructed. HCC cells in 12-well plates were introduced with reporter plasmids and miR-136-5p or miR-NC. The luciferase intensities were detected via commercial Dual-luciferase reporter assay system kit (Promega).

Animal study

BALB/c male nude mice acquired from Vital River Laboratory Animal Technology (Beijing, China) were arbitrarily allocated into two groups (n = 6). 5×10^6 Huh-7 cells stably expressing sh-NC, sh-circ_0091579#1, or sh-circ_0091579#2 were inoculated into the dorsal of nude mice. Tumor growth was recorded every week, and tumor volume was analyzed using the equation of length $\times$ width^2 $\times$ 0.5. After 4-week injection, these mice were killed and the tumors were weighed. The protein abundance of proliferation marker Ki67 was detected by immunohistochemistry (IHC) assay using the antibody of Ki67 (ab15580; 1:600; Abcam) [21]. Animal experiment was carried out with the approval of the Animal Research Committee of Yantaishan Hospital of Shandong Province.

Statistical analysis

GraphPad Prism 7.0 software (GraphPad, La Jolla, CA, USA) with the method of Student's *t*-test or one-way analysis of variance (ANOVA) were utilized to analyze data. Each experiment was conducted for at least three times. Results were expressed as the form of mean ± standard deviation (SD). Linear correlation was assessed using Spearman's correlation coefficient. Five-year survival rate curve of HCC patients was generated by Kaplan–Meier plot and analyzed by log-rank test. *p*-value <0.05 was considered as significant difference.

Results

Circ_0091579 is dysregulated in HCC tissues and cell lines

Circ_0091579 is derived from the back-splicing of exon 5–9 of its host gene GPC3, whose mature spliced sequence length is 1145 nt (Supplementary Figure 1A). Circ_0091579 can be amplified by divergent primers in cDNA group but not that of gDNA group (Supplementary Figure 1B), suggesting that circ_0091579 is a circular transcript. The expression pattern of circ_0091579 was analyzed in HCC. Circ_0091579 expression

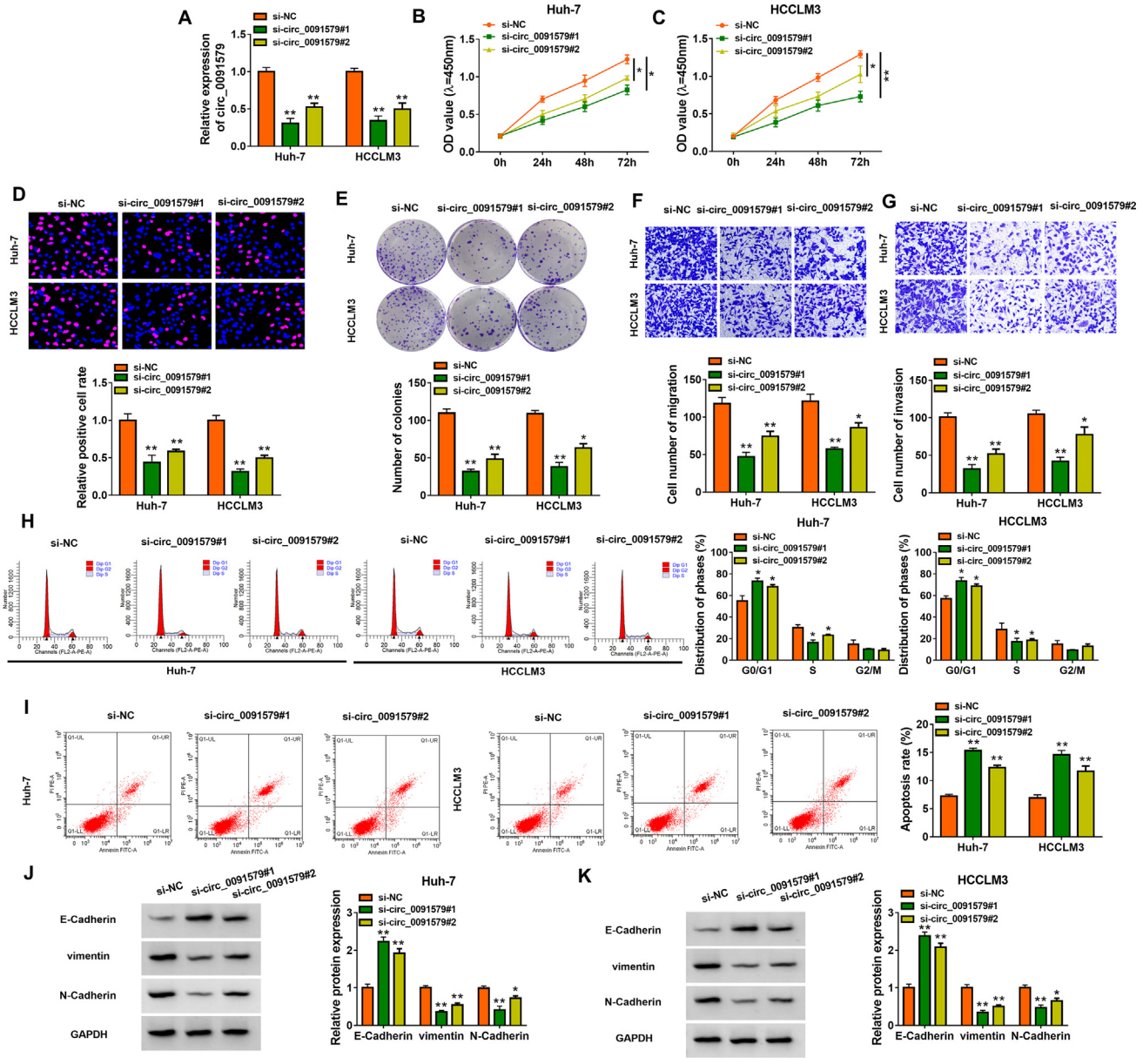

Fig. 2 **Circ_0091579 knockdown blocks the proliferation, migration, invasion, cell cycle progression and EMT and induces the apoptosis of HCC cells.** (A–K) HCC cells were transfected with si-NC, si-circ_0091579#1, or si-circ_0091579#2. (A) The relative level of circ_0091579 was determined in transfected HCC cells by RT-qPCR. (B and C) CCK8 assay was applied to analyze the proliferation capacity of circ_0091579-silenced HCC cells. (D) EdU assay was performed to assess the proliferation ability of circ_0091579-silenced HCC cells. (E) Cell proliferation ability was analyzed via colony formation assay. (F and G) Transwell assays were carried out to evaluate cell migration and invasion abilities. (H) The distribution of HCC cells in different phases (G0/G1, S and G2/M) of cell cycle progression was analyzed by flow cytometry. (I) Cell apoptosis rate ($FITC^{+}$ and $PI^{+/-}$) was analyzed by flow cytometry. (J and K) The expression of EMT-associated markers (E-Cadherin, vimentin and N-Cadherin) was measured by Western blot assay. $*p < 0.05$, $**p < 0.01$.

was higher in HCC tissues (n = 70) and cell lines compared with ANT tissues (n = 70) and THLE-2 cell line (Fig. 1A and B). We analyzed the association between circ_0091579 expression and the survival rate of 35 HCC patients. HCC patients were split into high circ_0091579 expression group (n = 16) and low circ_0091579 expression group (n = 17) with the median expression level of circ_0091579 as the cutoff. HCC patients with high expression of circ_0091579 was associated with low five-year survival rate (Fig. 1C). In addition, HCC patients with high expression of circ_0091579 were associated with advanced TNM stage and large tumor size (Table 1), further indicating the potential of circ_0091579 to be a novel prognostic biomarker in HCC patients. The circular structure of circ_0091579 was tested with exonuclease RNase R. The results showed that the level of the linear form of circ_0091579 (GPC3) was notably reduced upon RNase R degradation, while circ_0091579 was resistant to RNase R treatment (Fig. 1D and E), indicating that circ_0091579 was a circular transcript.

These results demonstrated that circ_0091579 might be a crucial regulatory factor in HCC progression.

Circ_0091579 knockdown blocks the proliferation, migration, invasion, cell cycle progression and epithelial–mesenchymal transition (EMT) and induces the apoptosis of HCC cells

We silenced endogenous circ_0091579 using si-circ_0091579#1 and si-circ_0091579#2 to analyze the phenotypes of HCC cells. The results of RT-qPCR confirmed the high silencing efficiency of si-circ_0091579#1 and si-circ_0091579#2 in HCC cells (Fig. 2A). Cell proliferation was markedly restrained in circ_0091579-silenced HCC cells compared with that in si-NC-transfected HCC cells (Fig. 2B and C). The rate of EdU^+ cells was markedly reduced with the knockdown of circ_0091579 relative to si-NC group (Fig. 2D). The number of colonies was also decreased in circ_0091579-silenced group than that in si-NC group (Fig. 2E). These results suggested that circ_0091579 knockdown suppressed the proliferation of HCC cells. The numbers of migrated and invaded cells were notably reduced with the silencing of circ_0091579 (Fig. 2F and G), indicating that circ_0091579 silencing inhibited the motility of HCC cells. Circ_0091579 knockdown reduced the percentage of HCC cells in S phase but increased the percentage in G0/G1 phase (Fig. 2H), suggesting that circ_0091579 interference suppressed cell cycle progression from G1 phase to S phase. Circ_0091579 silencing notably increased the percentage of apoptotic HCC cells (Fig. 2I). Three EMT-associated markers were detected by Western blot assay to analyze the effect of circ_0091579 silencing on the EMT of HCC cells. As shown in Fig. 2J and K, circ_0091579 silencing reduced the protein expression of vimentin and N-Cadherin and increased the level of E-Cadherin, indicating that circ_0091579 interference suppressed EMT of HCC cells. Overall, circ_0091579 silencing suppressed the malignant behaviors of HCC cells.

Circ_0091579 acts as miR-136-5p sponge in HCC cells

The subcellular localization of circ_0091579 was analyzed in HCC cells. Similar to GAPDH, circ_0091579 mainly located in the cytoplasm of HCC cells (Fig. 3A and B), which gave it the potential to act as miRNA sponge in cytoplasm. Based on the expression pattern of circ_0091579 in HCC, its interacted

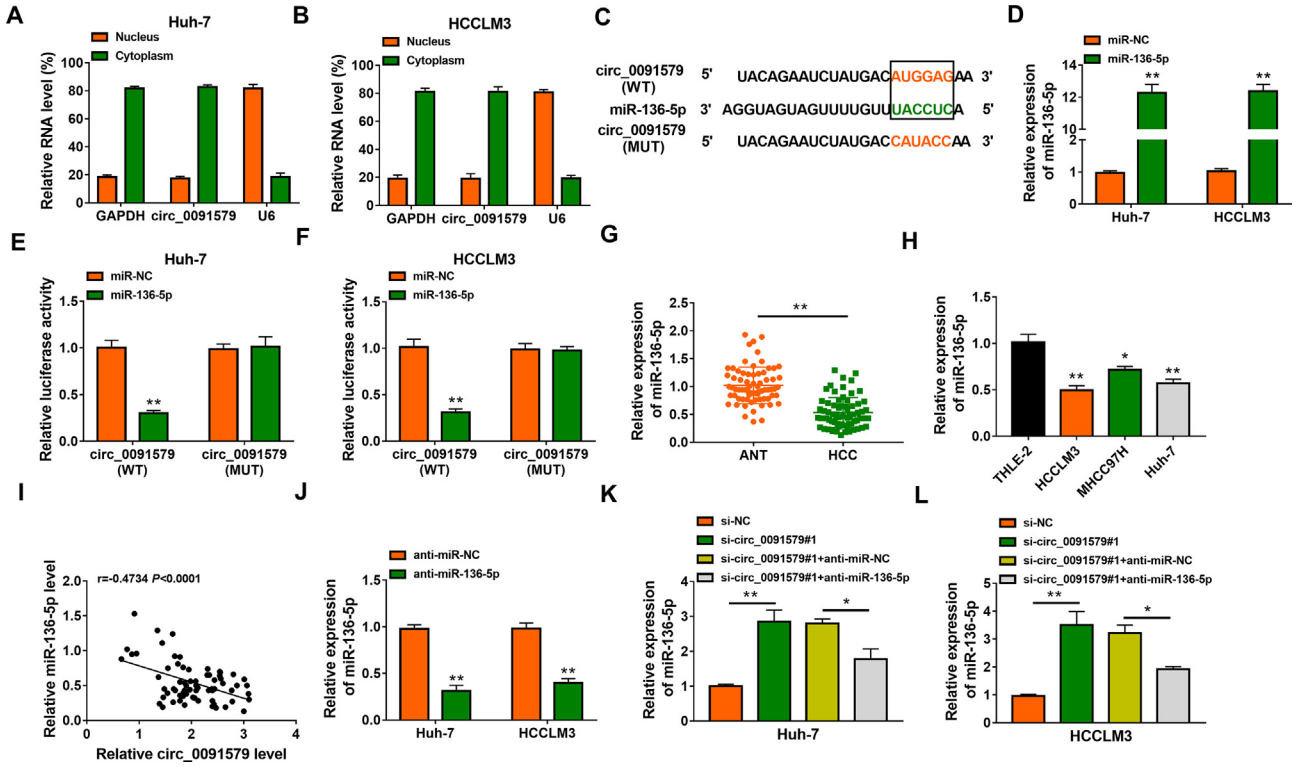

Fig. 3 **Circ_0091579 acts as miR-136-5p sponge in HCC cells.** (A and B) The subcellular distribution of circ_0091579 in the nucleus and cytoplasm of HCC cells was analyzed. (C) The putative binding sites of miR-136-5p in circ_0091579 predicted by bioinformatics database CircInteractome were shown. (D) RT-qPCR was applied to analyze the overexpression efficiency of miR-136-5p mimics in HCC cells. (E and F) The target relation between miR-136-5p and circ_0091579 was verified through conducting dual-luciferase reporter assay. (G) RT-qPCR was employed to assess the level of miR-136-5p in HCC tissues (n = 70) and ANT tissues (n = 70). (H) The expression level of miR-136-5p was determined in HCC cell lines and THLE-2 by RT-qPCR. (I) The linear correlation between miR-136-5p level and circ_0091579 level was analyzed by Spearman's correlation coefficient. (J) The silencing efficiency of miR-136-5p inhibitor (anti-miR-136-5p) was analyzed by RT-qPCR. (K and L) Huh-7 and HCCLM3 cells were transfected with si-NC, si-circ_0091579#1, si-circ_0091579#1 + anti-miR-NC or si-circ_0091579#1 + anti-miR-136-5p. The relative expression of miR-136-5p was determined in transfected HCC cells by RT-qPCR. *$p < 0.05$, **$p < 0.01$.

miRNAs should exhibit low expression in HCC. Through bioinformatics prediction using CircInteractome database and literature review, we focused on eight candidate miRNAs, including miR-1225-5p [22], miR-1287 [23], miR-1299 [24], miR-653 [25], miR-136-5p [12–14], miR-623 [26], miR-591 [27], and miR-630 [28]. Circ_0091579 silencing significantly up-regulated the expression of miR-653, miR-136-5p, and miR-630 in both HCC cell lines (Supplementary Fig. 2A and 2B), especially miR-136-5p. Therefore, we further tested the interaction between circ_0091579 and miR-136-5p in HCC cells. The putative binding sites between circ_0091579 and miR-136-5p were shown in Fig. 3C. Overexpression efficiency of miR-136-5p mimics was high in HCC cells (Fig. 3D). With the overexpression of miR-136-5p, the luciferase intensity of luciferase reporter plasmid circ_0091579 (WT) was markedly reduced compared with miR-NC-transfected group (Fig. 3E and F). The luciferase intensity of luciferase reporter plasmid circ_0091579 (MUT) which contained the mutant binding sites with miR-136-5p was unaffected with the transfection of miR-136-5p or miR-NC (Fig. 3E and F), indicating that circ_0091579 bound to miR-136-5p via the predicted binding sites. MiR-136-5p expression was markedly reduced in HCC tissues and cell lines relative to ANT tissues and THLE-2 cell line (Fig. 3G and H). MiR-136-5p expression in HCC tissues was negatively correlated with circ_0091579 expression (Fig. 3I). Through Northern blot, we found that the knockdown efficiencies of si-circ_0091579#1, si-circ_0091579#2, and si-circ_0091579#3 were significant in Huh-7 cells (Supplementary Figure 3A), and miR-136-5p was negatively regulated by circ_0091579 (Supplementary Figure 3B). The results of RT-qPCR assay suggested that the silencing efficiency of anti-miR-136-5p was high in HCC cells (Fig. 3J). Circ_0091579 knockdown elevated miR-136-5p expression, and the expression of miR-136-5p was markedly reduced with the addition of anti-miR-136-5p (Fig. 3K and L). Taken together, circ_0091579 negatively regulated miR-136-5p expression in HCC cells through binding to it.

Circ_0091579 knockdown suppresses the malignant potential of HCC cells partly through up-regulating miR-136-5p

The effects of circ_0091579/miR-136-5p axis on the phenotypes of HCC cells were analyzed. Through conducting CCK8 assay, EdU assay and colony formation assay, we found that miR-136-5p silencing largely overturned circ_0091579 knockdown-mediated suppressive effect on the proliferation of HCC cells (Fig. 4A-D). The migration ability and invasion ability of circ_0091579-silenced HCC cells were also largely recovered with the introduction of anti-miR-136-5p (Fig. 4E and F). Cell cycle progression was suppressed in circ_0091579-silenced HCC cells, which was largely counteracted by the addition of anti-miR-136-5p (Fig. 4G and H). Circ_0091579

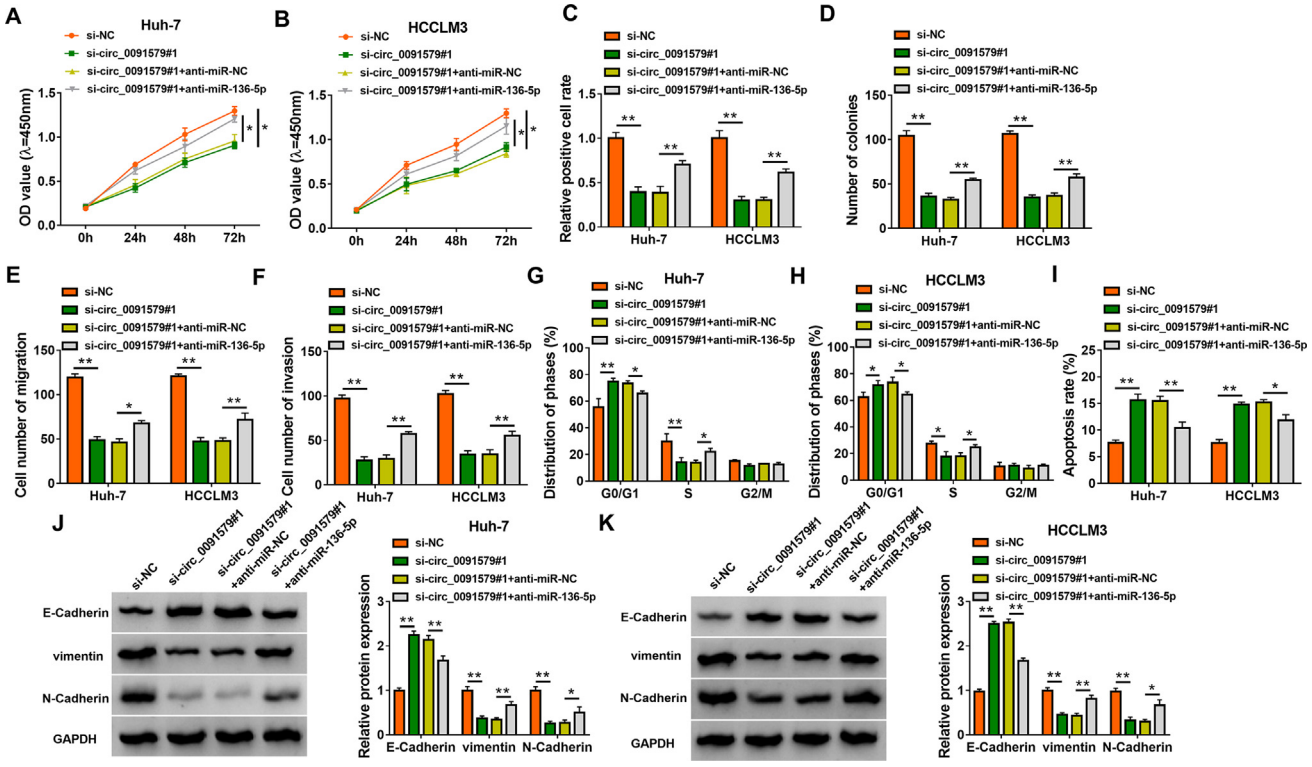

Fig. 4 **Circ_0091579 knockdown suppresses the malignant potential of HCC cells partly through up-regulating miR-136-5p.** (A–K) Huh-7 and HCCLM3 cells were transfected with si-circ_0091579#1 alone or together with anti-miR-136-5p. (A and B) CCK8 assay was applied to analyze cell proliferation. (C) EdU assay was conducted to analyze cell proliferation ability. (D) Colony formation assay was conducted to measure cell proliferation capacity. (E and F) Cell migration and invasion abilities were analyzed by transwell migration and invasion assays. (G and H) Cell cycle progression was detected by flow cytometry. (I) The apoptosis rate ($FITC^{+}$ and $PI^{+/-}$) was determined by flow cytometry. (J and K) The levels of EMT-associated markers were detected by Western blot assay. *$p < 0.05$, **$p < 0.01$.

interference-induced apoptosis in HCC cells was attenuated by the silencing of miR-136-5p (Fig. 4I). The expression of E-Cadherin was up-regulated by the silencing of circ_0091579, which was reduced with the silencing of miR-136-5p (Fig. 4J and K). The expression of vimentin and N-Cadherin exhibited a reverse tendency to E-Cadherin (Fig. 4J and K). These results demonstrated that circ_0091579 interference suppressed HCC development partly through up-regulating the anti-tumor molecule miR-136-5p.

MiR-136-5p negatively regulates TRIM27 expression via binding to it

Bioinformatics database TargetScan was utilized to predict the targets of miR-136-5p. Based on the expression pattern of miR-136-5p in HCC, its interacted mRNAs should exhibit high expression in HCC. Through bioinformatics prediction and literature review, we focused on six candidate mRNAs, including PAX6 [29], SEMA4C [30], ROCK1 [31], FZD4 [32], TRIM27 [20], and ABCC12 [33]. MiR-136-5p overexpression reduced the levels of FZD4, TRIM27, and ABCC12 in both HCC cell lines (Supplementary Fig. 2C and 2D), especially TRIM27. We further explored the binding relationship between miR-136-5p and TRIM27 in HCC cells. The putative binding sequence between miR-136-5p and TRIM27 was shown in Fig. 5A. The luciferase activity was markedly reduced in luciferase plasmid TRIM27 3′ untranslated region (3′UTR) (WT) group with the co-transfection of miR-136-5p relative to miR-NC group (Fig. 5B and C). However, luciferase intensity was unaffected in luciferase plasmid TRIM27 3′UTR (MUT) group with the co-transfection of miR-136-5p or miR-NC (Fig. 5B and C), suggesting the binding relation between miR-136-5p and TRIM27 in HCC cells. TRIM27 mRNA and protein expression was significantly up-regulated in HCC tissues relative to ANT tissues (Fig. 5D and E). Compared with human normal liver immortalized cell line THLE-2, TRIM27 was markedly up-regulated in three HCC cell lines (Fig. 5F). TRIM27 expression was negatively correlated with miR-136-5p expression (Fig. 5G). The expression of circ_0091579 was positively correlated with TRIM27 expression (Fig. 5H). Transfection with

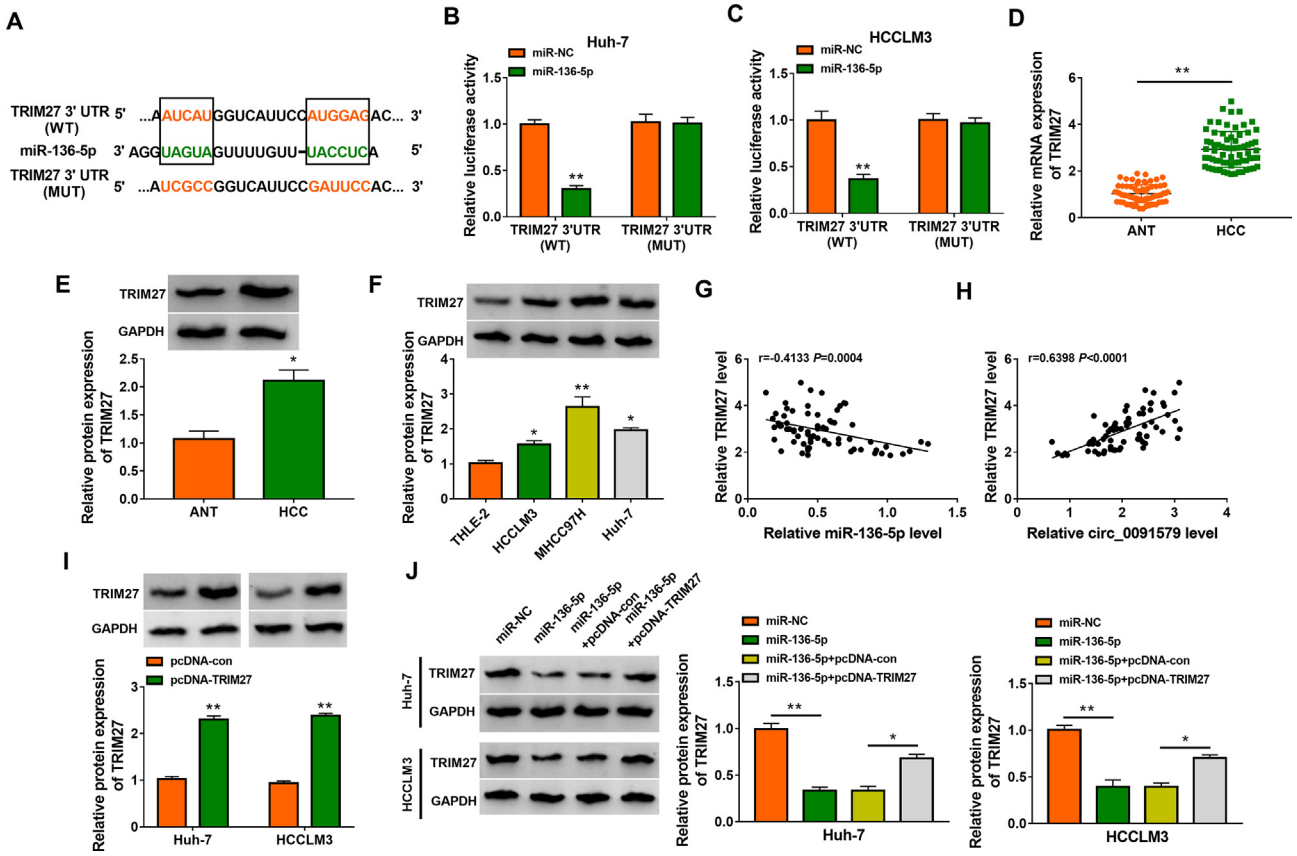

Fig. 5 **MiR-136-5p negatively regulates TRIM27 expression via binding to it.** (A) Bioinformatics database TargetScan was utilized to predict the downstream molecules of miR-136-5p, and TRIM27 was predicted as a possible target of miR-136-5p. The putative binding sites between miR-136-5p and TRIM27 were shown. (B and C) Dual-luciferase reporter assay was applied to test if TRIM27 was a binding partner of miR-136-5p. (D and E) The mRNA and protein expression of TRIM27 in HCC tissues and ANT healthy tissues was measured by RT-qPCR and Western blot assay, respectively. (F) Western blot assay was employed to analyze the protein expression of TRIM27 in HCC cell lines and THLE-2 cell line. (G and H) The linear correlation between the expression of TRIM27 and the expression of miR-136-5p or circ_0091579 was analyzed by Spearman's correlation coefficient. (I) The transfection efficiency of TRIM27 plasmid was assessed by Western blot assay. (J) The protein expression of TRIM27 was determined in Huh-7 and HCCLM3 cells transfected with miR-136-5p alone or together with pcDNA-TRIM27 by Western blot assay. $*p < 0.05$, $**p < 0.01$.

TRIM27 plasmid markedly up-regulated TRIM27 expression in HCC cells (Fig. 5I). MiR-136-5p overexpression down-regulated TRIM27 protein level (Fig. 5J), suggesting that miR-136-5p negatively regulated TRIM27 expression in HCC cells. The addition of TRIM27 plasmid largely rescued TRIM27 expression in miR-136-5p-overexpressed HCC cells (Fig. 5J). These findings suggested that miR-136-5p bound to the 3′UTR of TRIM27 in HCC cells.

MiR-136-5p overexpression restrains the malignant behaviors of HCC cells partly through reducing the expression of its target TRIM27

Through performing CCK8 assay, EdU assay and colony formation assay, we found that miR-136-5p overexpression prominently restrained the proliferation of HCC cells (Fig. 6A-D). MiR-136-5p overexpression suppressed the migration and invasion abilities of HCC cells (Fig. 6E and F). MiR-136-5p overexpression arrested cell cycle progression at G1/S transition (Fig. 6G and H). Cell apoptosis was triggered in miR-136-5p-overexpressed HCC cells (Fig. 6I). MiR-136-5p overexpression decreased the expression of vimentin and N-Cadherin and increased the level of E-Cadherin (Fig. 6J and K), indicating that the ectopic expression of miR-136-5p restrained the EMT of HCC cells. These results demonstrated that miR-136-5p exhibited an anti-tumor role in HCC cells. To explore if miR-136-5p exerted an anti-tumor role in HCC cells through targeting TRIM27, we co-transfected miR-136-5p and pcDNA-TRIM27 into HCC cells to perform compensation experiments. TRIM27 overexpression partly recovered the proliferation ability in miR-136-5p-overexpressed HCC cells (Fig. 6A-D). Cell migration and invasion abilities were partly rescued with the introduction of pcDNA-TRIM27 in miR-136-5p-overexpressed HCC cells (Fig. 6E and F). MiR-136-5p overexpression-induced cell cycle arrest was partly diminished by the introduction of TRIM27 ectopic expression plasmid (Fig. 6G and H). MiR-136-5p overexpression-induced cell apoptosis was partly attenuated by the accumulation of TRIM27 in HCC cells (Fig. 6I). The overexpression of TRIM27 suppressed the expression of E-Cadherin and up-regulated the expression of vimentin and N-Cadherin in miR-136-5p-overexpressed HCC cells (Fig. 6J and K). Overall, miR-136-5p exhibited an anti-tumor role in HCC cells partly through down-regulating TRIM27.

Circ_0091579 knockdown reduces TRIM27 partly through up-regulating miR-136-5p expression in HCC cells

Huh-7 and HCCLM3 cells were transfected with four groups: si-NC, si-circ_0091579#1, si-circ_0091579#1 + anti-miR-NC and si-circ_0091579#1 + anti-miR-136-5p. Circ_0091579 silencing reduced the expression of TRIM27, and the addition of anti-miR-136-5p partly rescued TRIM27 expression in HCC cells

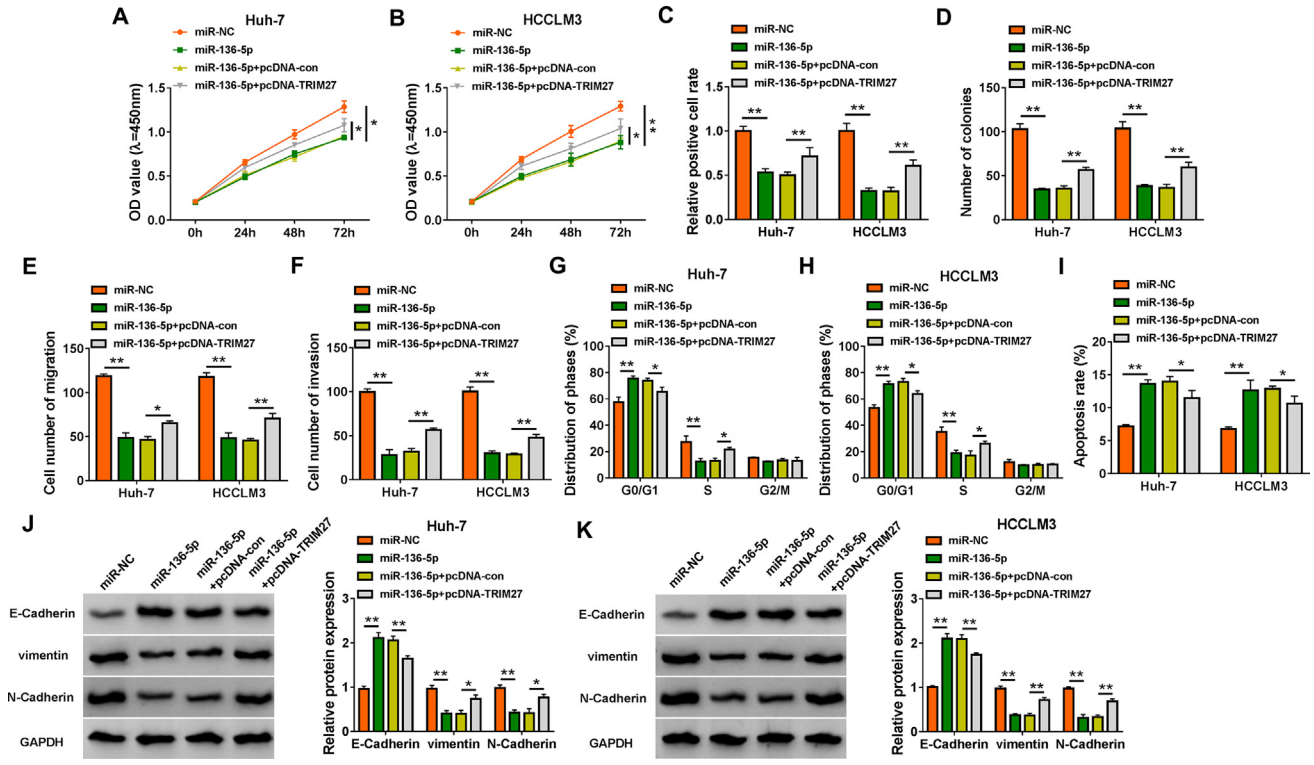

Fig. 6 **MiR-136-5p overexpression restrains the malignant behaviors of HCC cells partly through reducing the expression of its target TRIM27.** (A–K) Huh-7 and HCCLM3 cells were transfected with miR-136-5p alone or together with pcDNA-TRIM27. (A and B) CCK8 assay was employed to measure cell proliferation ability. (C) Cell proliferation ability was detected by EdU assay. (D) Colony formation assay was conducted to analyze the proliferation ability of HCC cells. (E and F) Cell motility was analyzed via transwell migration and invasion abilities. (G and H) Cell cycle progression was assessed by flow cytometry. (I) Flow cytometry was employed to analyze the apoptosis rate ($FITC^+$ and $PI^{+/-}$) of HCC cells. (J and K) The levels of E-Cadherin, vimentin and N-Cadherin were determined in transfected HCC cells by Western blot assay. $^*p < 0.05$, $^{**}p < 0.01$.

(Fig. 7A and B), suggesting that circ_0091579 acted as miR-136-5p sponge to up-regulate TRIM27 in HCC cells.

Circ_0091579 silencing suppresses HCC progression in vivo

Circ_0091579 knockdown significantly restrained xenograft tumor growth *in vivo* (Fig. 8A). The nude mice were humanely killed and xenograft tumors were resected. The tumors in sh-NC group, sh-circ_0091579#1 and sh-circ_0091579#2 groups were shown (Fig. 8B). Tumor weight was prominently reduced in xenograft tumors derived from circ_0091579-silenced Huh-7 cells (Fig. 8C). The expression of circ_0091579, miR-136-5p and TRIM27 protein was determined by RT-qPCR and Western blot assay. As shown in Fig. 8D and E, the expression of circ_0091579 and TRIM27 protein was markedly reduced in circ_0091579-silenced group than that in sh-NC group. There was an opposite expression tendency between the expression of miR-136-5p and circ_0091579 or TRIM27 in tumor tissues (Fig. 8D). The abundance of proliferation marker Ki67 in xenograft tumor samples was measured by IHC assay. As shown in Fig. 8F, circ_0091579 silencing reduced the level of Ki67 in tumor tissues. These findings suggested that circ_0091579 exerted a pro-tumor role in HCC *in vivo*.

Discussion

An increasing number of circRNAs have shown their "miRNA sponge" role to regulate initiation and progression of multiple malignancies [9,34]. For instance, circ_0008305 facilitated HCC progression via functioning as miR-660 sponge [35]. Circ-ZKSCAN1 restrained the progression of HCC through acting as the molecular sponge of miR-873-5p [36]. Circ_0001175 contributed to HCC development through sponging miR-130a-5p [37]. Circ_0091579 was identified to be an oncogene in liver cancer by previous studies [7,8,38]. Circ_0091579 abundance was significantly increased in HCC, and high level of circ_0091579 predicted a worse prognosis of HCC patients [7]. Circ_0091579 elevated malignant potential in HCC cells by mediating miR-490-5p/CASC3 signaling [8]. Niu et al. found that circ_0091579 enhanced the malignant capacities in liver cancer cells through absorbing miR-490-3p [38]. We found that circ_0091579 abundance was elevated in HCC, and HCC patients with high expression of circ_0091579 were correlated with short survival time. Additionally, through performing loss-of-function experiments, we found that circ_0091579 played an oncogenic role to accelerate the proliferation, migration, invasion, cell cycle progression and EMT and suppress the apoptosis of HCC cells.

Many miRNAs were dysregulated in HCC, and miRNAs served as oncogenes or tumor suppressors to regulate tumor development [39,40]. MiR-136-5p was verified as a tumor suppressor in many malignancies. For instance, circ_0003998 contributed to the development and Docetaxel resistance in non-small cell lung cancer through suppressing miR-136-5p [41]. Circ-TLK1 accelerated renal cell carcinoma development through inhibiting miR-136-5p [42]. Circ_100290 facilitated laryngeal squamous cell cancer development via

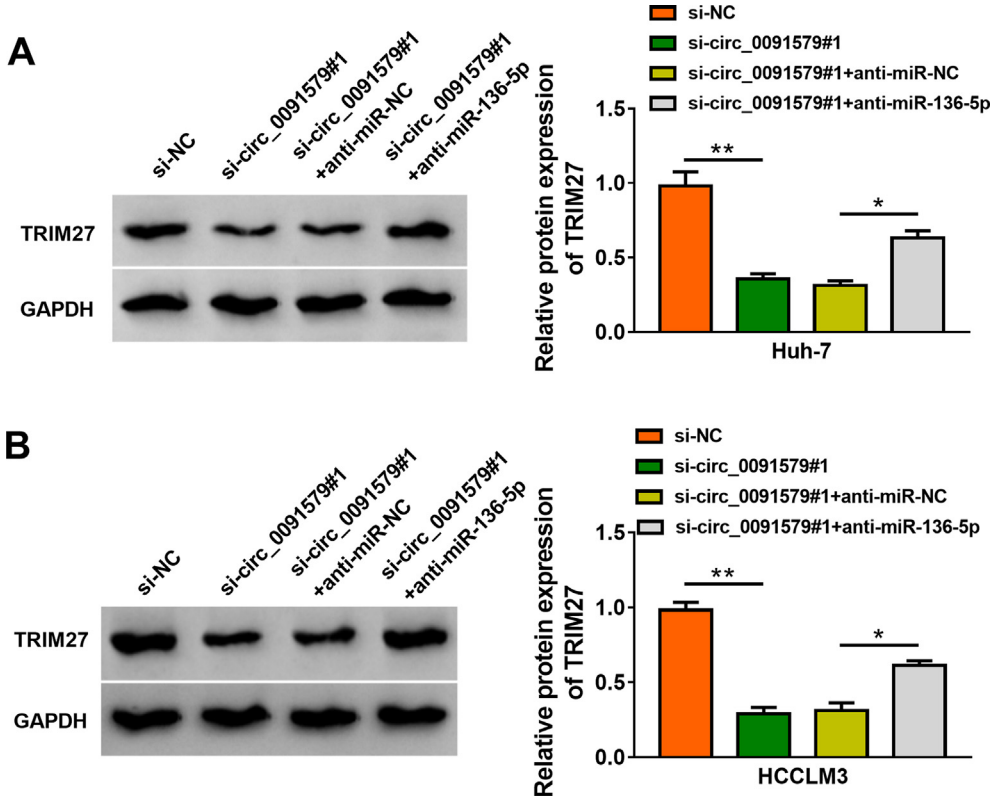

Fig. 7 **Circ_0091579 knockdown reduces TRIM27 partly through up-regulating miR-136-5p expression in HCC cells.** (A and B) Western blot assay was applied to determine the protein expression of TRIM27 in HCC cells transfected with si-circ_0091579#1 alone or together with anti-miR-136-5p. *$p < 0.05$, **$p < 0.01$.

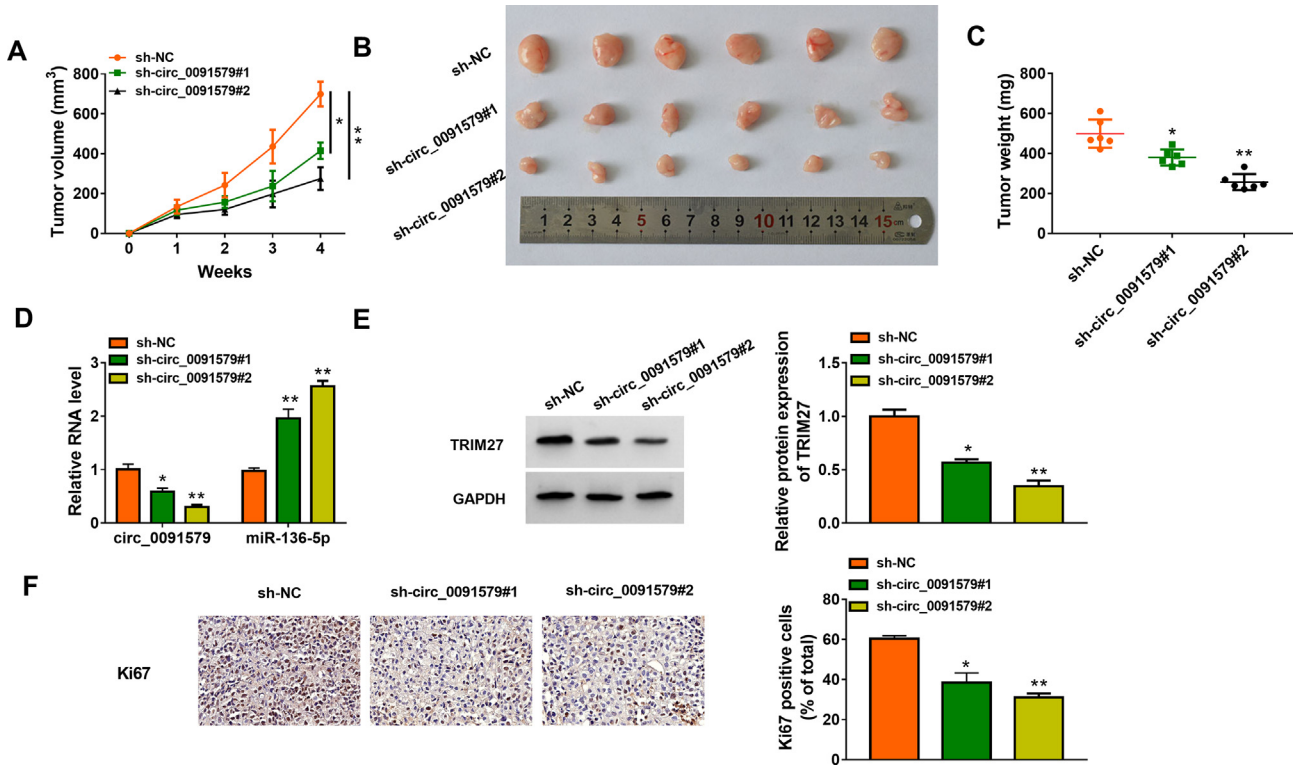

Fig. 8 **Circ_0091579 silencing suppresses HCC progression *in vivo*.** Huh-7 cells were subcutaneously inoculated into the nude mice (n = 6 in each group), and the growth of xenograft tumors was monitored. (A) Tumor volume was monitored every week. (B) The images of xenograft tumors in sh-NC, sh-circ_0091579#1, and sh-circ_0091579#2 groups were shown. (C) Tumor weight was recorded. (D and E) The levels of circ_0091579, miR-136-5p and TRIM27 in xenograft tumor tissues were measured by RT-qPCR and Western blot assay. (F) IHC assay was implemented to analyze the level of Ki67 in sh-NC, sh-circ_0091579#1, and sh-circ_0091579#2 groups. *$p < 0.05$, **$p < 0.01$.

suppressing miR-136-5p [43]. In HCC, Zhu et al. demonstrated that CRNDE enhanced the oncogenic phenotypes in HCC cells through up-regulating IRX5 via suppressing miR-136-5p [12]. Dong et al. demonstrated that LEF1-AS1 contributed to HCC development through suppressing miR-136-5p [13]. Circ_0091579 majorly located in the cytoplasmic fraction of HCC cells, implying its potential to sponge miRNAs. The target relation between circ_0091579 and miR-136-5p was verified. MiR-136-5p expression was prominently decreased in HCC. In addition, circ_0091579 negatively regulated miR-136-5p in HCC cells. Through performing compensation experiments, we found that circ_0091579 silencing suppressed the oncogenic phenotypes of HCC cells partly through elevating miR-136-5p expression.

TRIM27 contributed to non-small cell lung cancer development through modulating SIX3-β-catenin signaling pathway [44]. TRIM27 contributed to gastric cancer progression through activating Hippo-BIRC5 signaling [45]. TRIM27 facilitated the oncogenic properties in esophagus cancer cells through modulating PETN/AKT signaling [46]. As for HCC, Gao et al. demonstrated that TRIM27 acted as a downstream partner of miR-30 b-3p, and it accelerated malignant behaviors in HCC cells through activating PI3K/AKT signaling [20]. The binding between 3′UTR of TRIM27 and miR-136-5p was validated. Further assays indicated that miR-136-5p restrained the oncogenic properties in HCC cells partly through suppressing TRIM27. Subsequently, it was tested that circ_0091579 positively modulated TRIM27 abundance through functioning as a molecular sponge for miR-136-5p in HCC cells.

The *in vivo* role of circ_0091579 was consistent with its *in vitro* role in HCC cells. Through using xenograft tumor model, we found that circ_0091579 silencing restrained tumor growth *in vivo*.

There were some limitations in our study. The *in vivo* data regarding the role of circ_0091579 on the metastasis of HCC were lacking. Additionally, RNA-pull down assay and RNA immunoprecipitation assay need to be conducted in future to validate binding relation between miR-136-5p and circ_0091579 or TRIM27.

Our study demonstrated that circ_0091579 accelerated HCC progression via miR-136-5p-dependent regulation of TRIM27, which illustrated molecular mechanism behind the oncogenic function of circ_0091579 in HCC. Our study also provided novel potential therapeutic targets for HCC therapy.

Funding

None.

Conflicts of interest

The authors declare that they have no conflicts of interest.

Appendix A. Supplementary data

Supplementary data to this article can be found online at https://doi.org/10.1016/j.bj.2021.12.009.

REFERENCES

[1] Cidon EU. Systemic treatment of hepatocellular carcinoma: past, present and future. World J Hepatol 2017;9:797–807.
[2] Hartke J, Johnson M, Ghabril M. The diagnosis and treatment of hepatocellular carcinoma. Semin Diagn Pathol 2017;34:153–9.
[3] Ghouri YA, Mian I, Rowe JH. Review of hepatocellular carcinoma: epidemiology, etiology, and carcinogenesis. J Carcinog 2017;16:1.
[4] Lasda E, Parker R. Circular RNAs: diversity of form and function. RNA 2014;20:1829–42.
[5] Kristensen LS, Andersen MS, Stagsted LVW, Ebbesen KK, Hansen TB, Kjems J. The biogenesis, biology and characterization of circular RNAs. Nat Rev Genet 2019;20:675–91.
[6] Qu S, Yang X, Li X, Wang J, Gao Y, Shang R, et al. Circular RNA: a new star of noncoding RNAs. Cancer Lett 2015;365:141–8.
[7] Zhang C, Zhang C, Lin J, Wang H. Circular RNA Hsa_Circ_0091579 serves as a diagnostic and prognostic marker for hepatocellular carcinoma. Cell Physiol Biochem 2018;51:290–300.
[8] Liu W, Yin C, Liu Y. Circular RNA circ_0091579 promotes hepatocellular carcinoma proliferation, migration, invasion, and glycolysis through miR-490-5p/CASC3 Axis. Cancer Biother Radiopharm 2021;36:863–78.
[9] Panda AC. Circular RNAs act as miRNA sponges. Adv Exp Med Biol 2018;1087:67–79.
[10] Shu Z, Gao F, Xia Q, Zhang M. MiR-9-5p promotes cell proliferation and migration of hepatocellular carcinoma by targeting CPEB3. Biomarkers Med 2021;15:97–108.
[11] Cao X, Zhang J, Apaer S, Yao G, Li T. microRNA-19a-3p and microRNA-376c-3p promote hepatocellular carcinoma progression through SOX6-mediated Wnt/beta-catenin signaling pathway. Int J Gen Med 2021;14:89–102.
[12] Zhu L, Liu Y, Chen Q, Yu G, Chen J, Chen K, et al. Long-Noncoding RNA colorectal neoplasia differentially expressed gene as a potential target to upregulate the expression of IRX5 by miR-136-5P to promote oncogenic properties in hepatocellular carcinoma. Cell Physiol Biochem 2018;50:2229–48.
[13] Dong H, Jian P, Yu M, Wang L. Silencing of long noncoding RNA LEF1-AS1 prevents the progression of hepatocellular carcinoma via the crosstalk with microRNA-136-5p/WNK1. J Cell Physiol 2020;235:6548–62.
[14] Zheng Y, Chen CJ, Lin ZY, Li JX, Liu J, Lin FJ, et al. Circ_KATNAL1 regulates prostate cancer cell growth and invasiveness through the miR-145-3p/WISP1 pathway. Biochem Cell Biol 2020;98:396–404.
[15] Fabian MR, Sonenberg N, Filipowicz W. Regulation of mRNA translation and stability by microRNAs. Annu Rev Biochem 2010;79:351–79.
[16] Takahashi M, Ritz J, Cooper GM. Activation of a novel human transforming gene, ret, by DNA rearrangement. Cell 1985;42:581–8.
[17] Iwakoshi A, Murakumo Y, Kato T, Kitamura A, Mii S, Saito S, et al. RET finger protein expression is associated with prognosis in lung cancer with epidermal growth factor receptor mutations. Pathol Int 2012;62:324–30.
[18] Tsukamoto H, Kato T, Enomoto A, Nakamura N, Shimono Y, Jijiwa M, et al. Expression of Ret finger protein correlates with outcomes in endometrial cancer. Cancer Sci 2009;100:1895–901.
[19] Tezel GG, Uner A, Yildiz I, Guler G, Takahashi M. RET finger protein expression in invasive breast carcinoma: relationship between RFP and ErbB2 expression. Pathol Res Pract 2009;205:403–8.
[20] Gao D, Zhou Z, Huang H. miR-30b-3p inhibits proliferation and invasion of hepatocellular carcinoma cells via suppressing PI3K/Akt pathway. Front Genet 2019;10:1274.
[21] Yang Q, Yu W, Han X. Overexpression of microRNA101 causes antitumor effects by targeting CREB1 in colon cancer. Mol Med Rep 2019;19:3159–67.
[22] Liu L, Zhang W, Hu Y, Ma L, Xu X. Downregulation of miR-1225-5p is pivotal for proliferation, invasion, and migration of HCC cells through NFκB regulation. J Clin Lab Anal 2020;34:e23474.
[23] Lu J, Tang L, Xu Y, Ge K, Huang J, Gu M, et al. Mir-1287 suppresses the proliferation, invasion, and migration in hepatocellular carcinoma by targeting PIK3R3. J Cell Biochem 2018;119:9229–38.
[24] Zhu H, Wang G, Zhou X, Song X, Gao H, Ma C, et al. miR-1299 suppresses cell proliferation of hepatocellular carcinoma (HCC) by targeting CDK6. Biomed Pharmacother 2016;83:792–7.
[25] Zhang XW, Li QH, Xu ZD, Dou JJ. STAT1-induced regulation of lncRNA ZFPM2-AS1 predicts poor prognosis and contributes to hepatocellular carcinoma progression via the miR-653/GOLM1 axis. Cell Death Dis 2021;12:31.
[26] Wang M, Zhao H. LncRNA CTBP1-AS2 promotes cell proliferation in hepatocellular carcinoma by regulating the miR-623/cyclin D1 Axis. Cancer Biother Radiopharm 2020;35:765–70.
[27] Ji C, Hong X, Lan B, Lin Y, He Y, Chen J, et al. Circ_0091581 promotes the progression of hepatocellular carcinoma through targeting miR-591/FOSL2 Axis. Dig Dis Sci 2021;66:3074–85.
[28] Chen WX, Zhang ZG, Ding ZY, Liang HF, Song J, Tan XL, et al. MicroRNA-630 suppresses tumor metastasis through the TGF-β- miR-630-Slug signaling pathway and correlates inversely with poor prognosis in hepatocellular carcinoma. Oncotarget 2016;7:22674–86.
[29] Xu Q, Liu K. MiR-369-3p inhibits tumorigenesis of hepatocellular carcinoma by binding to PAX6. J Biol Regul Homeost Agents 2020;34:917–26.
[30] Yu Z, Du Y, Li H, Huang J, Jiang D, Fan J, et al. miR-642 serves as a tumor suppressor in hepatocellular carcinoma by regulating SEMA4C and p38 MAPK signaling pathway. Oncol Lett 2020;20:74.
[31] Li HW, Liu J. Circ_0009910 promotes proliferation and metastasis of hepatocellular carcinoma cells through miR-335-5p/ROCK1 axis. Eur Rev Med Pharmacol Sci 2020;24:1725–35.
[32] Yao X, You G, Zhou C, Zhang D. LncRNA ASB16-AS1 promotes growth and invasion of hepatocellular carcinoma through regulating miR-1827/FZD4 Axis And activating Wnt/β-catenin pathway. Cancer Manag Res 2019;11:9371–8.

[33] Borel F, Han R, Visser A, Petry H, van Deventer SJ, Jansen PL, et al. Adenosine triphosphate-binding cassette transporter genes up-regulation in untreated hepatocellular carcinoma is mediated by cellular microRNAs. Hepatology 2012;55:821–32.
[34] Kulcheski FR, Christoff AP, Margis R. Circular RNAs are miRNA sponges and can be used as a new class of biomarker. J Biotechnol 2016;238:42–51.
[35] Yan F, Fan B, Wang J, Wei W, Tang Q, Lu L, et al. Circ_0008305-mediated miR-660/BAG5 axis contributes to hepatocellular carcinoma tumorigenesis. Cancer Med 2021;10:833–42.
[36] Li J, Bao S, Wang L, Wang R. CircZKSCAN1 suppresses hepatocellular carcinoma tumorigenesis by regulating miR-873-5p/downregulation of deleted in liver cancer 1. Dig Dis Sci 2021;66:4374–83.
[37] Li L, He K, Chen S, Wei W, Tian Z, Tang Y, et al. Circ_0001175 promotes hepatocellular carcinoma cell proliferation and metastasis by regulating miR-130a-5p. OncoTargets Ther 2020;13:13315–27.
[38] Niu WY, Chen L, Zhang P, Zang H, Zhu B, Shao WB. Circ_0091579 promotes proliferative ability and metastasis of liver cancer cells by regulating microRNA-490-3p. Eur Rev Med Pharmacol Sci 2019;23:10264–73.
[39] Mizuguchi Y, Takizawa T, Yoshida H, Uchida E. Dysregulated miRNA in progression of hepatocellular carcinoma: a systematic review. Hepatol Res 2016;46:391–406.
[40] Chen E, Xu X, Liu R, Liu T. Small but heavy role: MicroRNAs in hepatocellular carcinoma progression. BioMed Res Int 2018;2018:6784607.
[41] Zhang W, Song C, Ren X. Circ_0003998 regulates the progression and Docetaxel sensitivity of DTX-resistant non-small cell lung cancer cells by the miR-136-5p/CORO1C Axis. Technol Cancer Res Treat 2021;20:1533033821990040.
[42] Li J, Huang C, Zou Y, Ye J, Yu J, Gui Y. CircTLK1 promotes the proliferation and metastasis of renal cell carcinoma by sponging miR-136-5p. Mol Cancer 2020;19:103.
[43] Wang Z, Huang C, Zhang A, Lu C, Liu L. Overexpression of circRNA_100290 promotes the progression of laryngeal squamous cell carcinoma through the miR-136-5p/RAP2C axis. Biomed Pharmacother 2020;125:109874.
[44] Liu S, Tian Y, Zheng Y, Cheng Y, Zhang D, Jiang J, et al. TRIM27 acts as an oncogene and regulates cell proliferation and metastasis in non-small cell lung cancer through SIX3-beta-catenin signaling. Aging 2020;12:25564–80.
[45] Yao Y, Liu Z, Cao Y, Guo H, Jiang B, Deng J, et al. Downregulation of TRIM27 suppresses gastric cancer cell proliferation via inhibition of the Hippo-BIRC5 pathway. Pathol Res Pract 2020;216:153048.
[46] Ma L, Yao N, Chen P, Zhuang Z. TRIM27 promotes the development of esophagus cancer via regulating PTEN/AKT signaling pathway. Cancer Cell Int 2019;19:283.